P H Y S I C A L   R E V I E W   L E T T E R S

Experimental Observation of Self-Accelerating Beams in Quadratic Nonlinear Media

Ido Dolev,[1] Ido Kaminer,[2] Asia Shapira,[1] Mordechai Segev,[2] and Ady Arie[1,*]

[1]*Department of Physical Electronics, Fleischman Faculty of Engineering, Tel-Aviv University, Tel-Aviv 69978, Israel*
[2]*Physics Department and Solid State Institute, Technion, Haifa 32000, Israel*

We present the experimental observation of 1D and 2D self-accelerating nonlinear beams in quadratic media, which are also the first nonlinear self-accelerating beams in any symmetric nonlinearity. Notably, we show that the intensity peaks of the first and second harmonics are asynchronous with respect to one another, but the coupled harmonics exhibit joint acceleration within the nonlinear medium. Finally, we demonstrate the impact of self-healing effects on the jointly accelerating first and second harmonics.

Self-accelerating optical beams have been attracting a great deal of interest since 2007, when Christodoulides and his co-workers introduced 30 year old ideas of self-accelerating quantum particles [1] into the domain of electromagnetic waves [2] and performed the first experiments [3]. Ideally, these beams propagate in a parabolic trajectory (thus they are "accelerating" in the transverse plane as they propagate) without changing their archetypical Airy-type structure while, in addition, displaying "self-healing" properties [4]. However, such beams carry infinite power; hence, in reality the beams have to be truncated. This implies that the beam can accelerate and approximately maintain its structure for a finite distance only, yet physically this distance can be very large (many diffraction lengths) [2,3]. Interestingly, relaxing the propagation-invariance requirement allows a beam of finite width to propagate along any convex trajectory [5]. All of these features make these self-accelerating beams useful for a variety of applications, e.g., manipulation of small particles [6], generation of curved plasma channels in air [7], generation of linear light bullets [8,9], and more.

Notwithstanding the progress with accelerating beams in linear optics, it is already clear that the next challenges are in nonlinear media. This Letter addresses self-accelerating nonlinear beams in quadratic media, giving rise to a second-order power exchange between fields of different frequencies. To date, experiments with Airy beams in quadratic media include the generation and manipulation of Airy beams through engineered periodic poling [10–12] and three-wave mixing of Airy beams [13–15]. In all of these experiments with Airy beams in quadratic media [10–13], the propagation in the nonlinear crystal was never shape-preserving; rather, the quadratic medium was used only as a means to generate Airy beams, which can exhibit shape-preserving acceleration in linear media (such as free space) but not in the nonlinear crystal where they were generated. Can nonlinearly coupled beams of different frequencies exhibit shape-preserving acceleration inside the nonlinear medium that supports their coupling?

This question becomes more profound by recalling the concept of quadratic solitons: optical beams comprised of two (or three) fields that jointly trap and balance their diffraction broadening. Quadratic solitons have been known for decades [16,17], yet to date they were always observed to propagate with a constant transverse velocity, that is, at a straight line normal to their phase front. However, a recent theory paper predicted that quadratic nonlinearities can support self-accelerating self-trapped beams: accelerating beams comprised of two (or three) different frequencies that propagate at a joint curved trajectory and are mutually trapped (by virtue of the nonlinearity) such that they exhibit shape-preserving propagation in the accelerated frame. Thus far, accelerating quadratically self-trapped beams have never been observed.

In this Letter, we present the first experimental observation of 1D and 2D self-accelerating nonlinear beams in quadratic media, which are also the first nonlinear self-accelerating beams in any symmetric nonlinearity. In the 1D case, we find perfect agreement with the theory [18], highlighting features such as intensity peaks of the first and second harmonics that are asynchronous with one another and mutual acceleration at a joint trajectory. We find experimentally that extending these ideas to 2D yields surprising phenomena which are very different from straightforward extension of the 1D result. Namely, launching a 2D Airy beam at the first harmonic (FH) gives rise to a second harmonic (SH) 2D Airy beam centered at the main lobe of the FH, along with some additional structure, emerging together from the quadratic crystal. This additional structure exhibits intriguing properties in free space, as the beam diffracts away from the crystal. Namely, after some distance, the beam transforms into two orthogonally structured 1D Airy beams and an additional semi-Gaussian beam. Finally, we demonstrate the self-healing properties of these nonlinear jointly accelerating beams with a 2D Airy beam whose central lobe was removed. The experiments show that these nonlinear beams, which are jointly trapped and jointly accelerating, can compensate for considerable perturbations in their structure.

Let us begin with the theory. Consider the paraxial phase-matched propagation of two coupled beams $\psi^{(1)}$ and $\psi^{(2)}$ at the first and second harmonics, respectively:

$$i\psi_z^{(1)} + \frac{1}{2k}\nabla_\perp^2 \psi^{(1)} + k\eta_1\psi^{(2)}(\psi^{(1)})^* = 0,$$

$$i\psi_z^{(2)} + \frac{1}{4k}\nabla_\perp^2 \psi^{(2)} + 2k\eta_2(\psi^{(1)})^2 = 0. \quad (1)$$

k is the FH wave number, and η_1 and η_2 are the effective nonlinear coupling coefficients of the FH and SH beams (proportional to $\chi^{(2)}$). As was done in Ref. [18], seeking coupled beams propagating along a parabolic trajectory simplifies the system considerably (although other trajectories may also exist [5]), giving two coupled equations for the shape-preserved amplitudes. We take similar dimensionless units as in Ref. [18] and assume the nondepleted pump approximation, to reach the equation for the SH, for the 1D and the 2D cases separately:

$$U_2''/4 - XU_2 = -2U_1^2,$$

$$\nabla_\perp^2 U_2/4 - (X+Y)U_2 = -2U_1^2,$$

$$U_1 \propto \text{Ai}(X) \quad (1D), \qquad U_1 \propto \text{Ai}(X)\text{Ai}(Y) \quad (2D). \quad (2)$$

U_1 and U_2 are the normalized amplitudes of the FH and SH beams, and X and Y are normalized transverse coordinates in the jointly accelerating frame. The solution for each of Eqs. (2) comprises of homogenous and inhomogenous parts. The homogenous part of the solution is proportional to $\text{Ai}(2^{2/3}X)$ and to $\text{Ai}(2^{2/3}X)\text{Ai}(2^{2/3}Y)$, for 1D and 2D, respectively. This homogeneous term, in both 1D and 2D, predicts that the oscillations in the structure of the SH should be $2^{2/3} \approx 1.587$ times faster than the structural oscillations in the pump. The inhomogeneous part of the solution has major differences between the 1D and the 2D cases. In 1D, this inhomogeneous term can be found in an integral form. For sufficiently strong nonlinear coupling [18], the variations of the inhomogenous part are much slower than those of the homogenous part, and therefore it can be considered as an envelope for the fast variation of the homogenous part. This envelope exhibits a tail that seems not to decay even asymptotically at large negative X. Moreover, at high pump intensities the envelopes of the FH and SH beams exhibit asynchronous oscillations, displaying the same ratio of $2^{2/3}$ as for the homogeneous term. As such, we expect the SH to have several strong peaks of similar height at large negative X, even in the case of a finite beam. As for the inhomogeneous term in 2D, the solution has to be found numerically, under boundary conditions for positive X (or Y). As shown below, these predicted features of the self-accelerating quadratic beams are apparent in the experimental results.

We now proceed to describe the experiments. Obviously, we chose the self-accelerating beam for our experiments to be a truncated Airy beam. In order to convert the fundamental Gaussian beam of the laser into a truncated Airy

beam, we can rely on the fact that the Fourier transform of the truncated Airy function is a Gaussian function with a cubic phase. For achieving this cubic phase modulation, we have fabricated two binary phase gratings that impose either 1D or 2D cubic modulations [19]. The grating profile for the 2D modulation is

$$h(X, Y) = \frac{1}{2}h_0\left\{\text{sgn}\left[\cos\left(\frac{2\pi}{\Lambda}X + aX^3 + bY^3\right)\right] + 1\right\}, \quad (3)$$

whereas for the 1D modulation we simply set $b = 0$. The required pattern is then observed in the first diffraction order of this grating, and it can be Fourier transformed into an Airy beam by using a lens. We fabricated the $10 \times 10 \text{ mm}^2$ phase masks on a silicon wafer by standard photolithography through a mask with the desired pattern, followed by aluminum evaporation, liftoff of the photoresist, and a deep reactive-ion etching process. This already provided a grating with the desired pattern on the Si surface, but, in order to improve its reflectivity, a 70 nm of silver layer was then evaporated on the silicon wafer. The cubic parameters in the phase masks, $a = b = 2 \times 10^{-8}[\mu\text{m}^{-3}]$, were designed to impose cubic phase modulation spanning over $\sim343\pi$ rad in our experimental conditions. This is a much larger phase span with respect to the span that is provided by a spatial light modulator.

The experimental setup consists of a Nd:YLF pump laser (1.0475 μm, 3 kHz repetition rate, and 7.62 ns pulse width) which is collimated to a waist diameter of 6 mm incident upon the 1D or 2D phase mask. The reflected light at the first diffraction order is then Fourier transformed with a lens, thereby generating an Airy beam. The Airy beam is imaged with a $4f$ system (magnification of 0.8) into a 10 mm long periodically poled KTiOPO4 crystal.
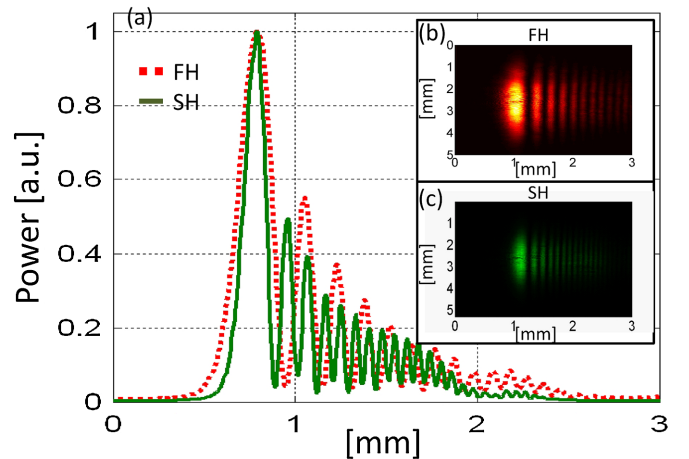

FIG. 1 (color online). Experimental results displaying the mutually asynchronous structures of the 1D FH and SH jointly accelerating beams. The SH beam oscillates at a higher frequency, with peaks located in both the peaks and the valleys of the 1D Airy FH. (a) Cross sections of the SH beam (solid line) and the FH (dashed line). Full frame of the FH (b) and SH (c) beams.

The nonlinear crystal, with a poling period of 8.5 μm, is held at the experimental phase matching temperature of $52.5 \pm 0.1\,°$C. After the crystal, the FH or the SH are filtered, and the output beam is imaged with another $4f$ system (magnification of 5.3) on a CCD camera placed on a rail. Under these conditions, the entire angular spectrum of the beam is within the angular acceptance of the crystal [20].

First we generate the 1D accelerating Airy beam. Using a FH beam with an average power of 7.16 mW, we measure the SH beam with an average power of 0.24 mW, giving an internal conversion efficiency of 1.41×10^{-4} W^{-1} (for the peak power), after accounting for the Fresnel reflections at the uncoated crystal facets. We then record the output beams after the periodically poled KTiOPO4 crystal. Since the energy transfer from the FH to the SH is relatively low, the output FH after the crystal essentially remains a 1D Airy beam [Fig. 1(b)]. The SH beam recorded after the crystal is shown in Fig. 1(c). It can be seen [Fig. 1(a)] that the SH beam has an Airy-like shape, yet it oscillates faster than the FH Airy beam, as predicted in the analytical calculations. As the FH and the SH are

jointly accelerating, the peaks of the main lobes of the FH and SH accelerate along the same trajectory (not shown). We emphasize that the peaks of the SH beam are located both in the peaks and in the dips of the original FH beam, even at places where the intensity of the FH is zero. This unique phenomenon occurs due to the joint acceleration of the beams (both FH and SH) inside the nonlinear crystal. This is also a proof of concept that these beams exhibit joint trapping by virtue of the quadratic nonlinearity, in a fashion similar to that supporting quadratic solitons. The experimental results are in agreement with the theoretical predictions [18].

Next, we study the case of a 2D accelerating Airy beam. Notably, we observed surprising phenomena which are very different from a straightforward extension of the 1D result. Figure 2 presents three frames in the propagation path: immediately after the crystal, and 20 and 50 cm after the crystal, for both for the FH and the SH. The FH has the expected propagation properties of 2D Airy beam: It accelerates and almost does not diffract [Figs. 2(a)–2(c)]. On the other hand, the SH beam is composed of several different structures that interfere together: It contains a 2D
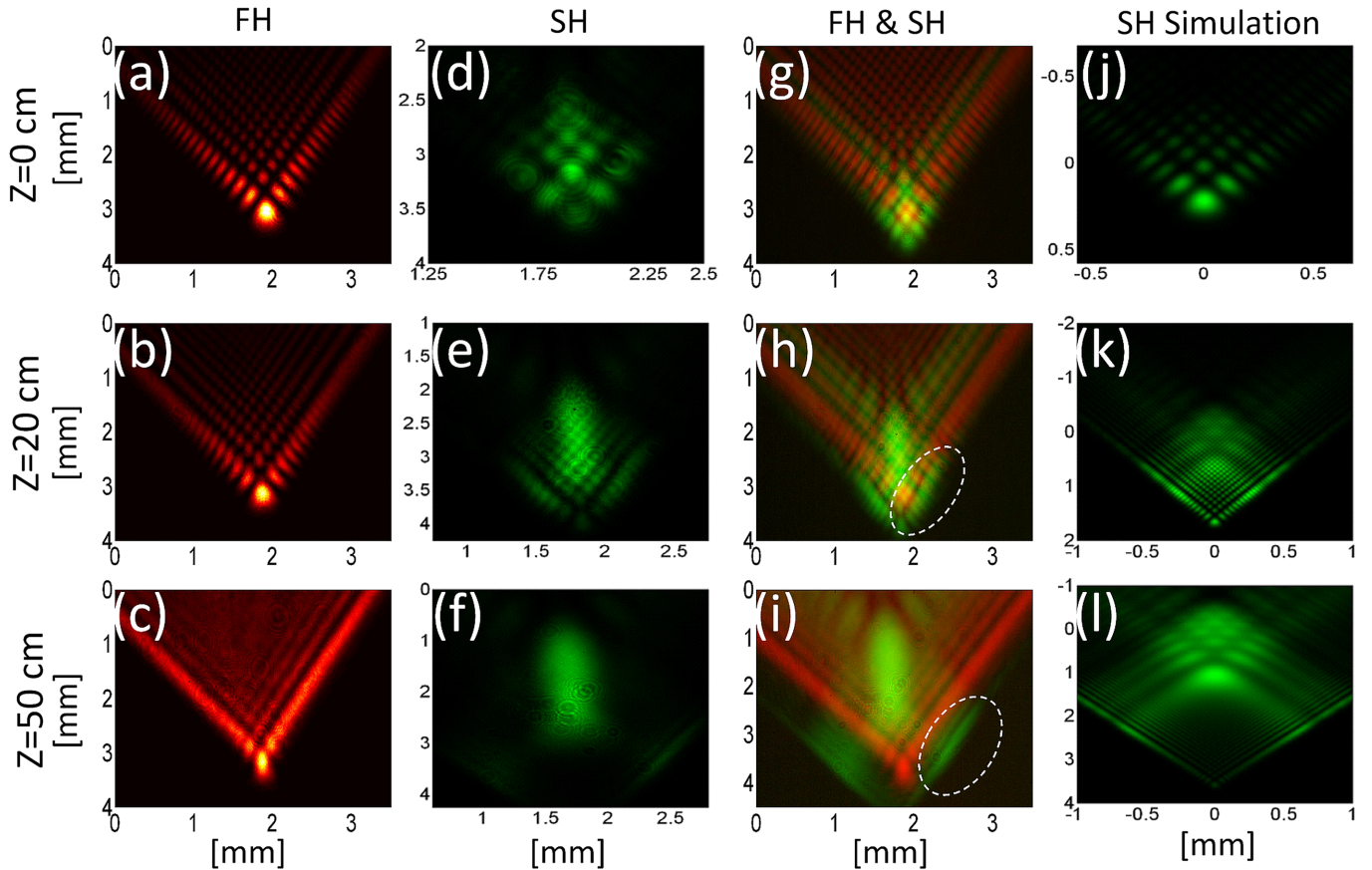

FIG. 2 (color online).   FH, red; SH, green. Experimental (a)–(i) and numerical (j)–(l) structures of the 2D beams emerging when a 2D Airy FH beam is launched. The beams are measured at the crystal exit face (a),(d),(g), after 20 cm (b),(e),(h), and after 50 cm (c), (f),(i). The combined FH and SH are presented on a log scale (g)–(i), where the dashed circles mark one of the 1D Airy structure. Panels (j)–(l) present the corresponding simulated results.

Airy beam, two 1D orthogonally structured Airy beams, and an additional semi-Gaussian beam. Right after the crystal, all these structures are mixed together [Fig. 2(d)], but after some distance the "modes" separate, each propagating in a different direction and at a different acceleration. The 2D Airy component accelerates downwards in the vertical direction of Figs. 2(d)–2(f), whereas the two orthogonally structured 1D Airy components accelerate diagonally in $\pm 45°$ and the semi-Gaussian part goes almost straight [Figs. 2(e) and 2(f)]. Each of these components carries a different amount of power and exhibits a different acceleration slope. Whereas immediately after the crystal the 2D Airy beam is dominant [Fig. 2(d)], after 20 cm the two 1D Airy and the semi-Gaussian modes become dominant [Figs. 2(e) and 2(f)].

We compare our experimental results to numerical simulations, carried out by the split-step Fourier method with the parameters of our experiments. The trends in the simulation results [Figs. 2(j)–2(l)] conform well to the experimental measurements. Figure 3 displays the measurements and the parabolic fits of the trajectory for each component. The FH and the SH 2D Airy beams are jointly accelerating, with parabolic coefficients of $5.16 \times 10^{-6} \pm 0.1 \times 10^{-6}[1/mm]$ and $5.3 \times 10^{-6} \pm 0.1 \times 10^{-6}[1/mm]$, respectively. The orthogonal 1D Airy components have lower acceleration $(3.74\text{-}6 \pm 0.1 \times 10^{-6}[1/mm]$ and $3.54 \times 10^{-6} \pm 0.1 \times 10^{-6}[1/mm])$, roughly $\sqrt{2}$ times lower than the acceleration of the 2D Airy beam (as the theory predicts). The semi-Gaussian part essentially does not accelerate. We emphasize that the two 1D Airy beams and the semi-Gaussian structure, both emerging from the nonlinear crystal in the 2D experiment, arise from the inhomogeneous part of the solution of Eq. (2). Namely, the inhomogeneous term is shape-preserving only in the quadratic medium: After it exits the crystal, it experiences diffraction broadening and transforms into the two 1D Airy

beams and a semi-Gaussian structure, as observed in Figs. 2 and 3.

We also study the self-healing properties of the FH and SH. For this purpose, we block the main lobe of the 2D Airy beam pump by using a sharp knife [Fig. 4(a)] and measure the output beams after the nonlinear crystal. Because of the self-healing property of the Airy beam, the main lobe of the FH is already regenerated while propagating in the nonlinear crystal. Just after the crystal, the FH has recovered its full 2D Airy shape [Fig. 4(b)], as expected, because our experiments are in the non-depleted-pump regime. The SH beam is presented in Fig. 4(d). Surprisingly, when the main lobe of the FH is blocked, the resultant SH beam is much more similar to a 2D Airy beam than when the full 2D Airy FH is launched [i.e., compare Figs. 4(d) and 2(d)]. Notably, the SH 2D Airy component is now more pronounced and contains more power than the semi-Gaussian component. The FH and SH nonlinear beams, which are jointly trapped and jointly accelerating, compensate for considerable perturbations in their initial structure. While propagating, the two 1D Airy beams appear again, as shown in Fig. 4(e). This suggests that the main contribution from the main lobe of the FH beam to the SH beam is to the semi-Gaussian part, whereas the 2D and 1D Airy beams arise from the side lobes of the FH. This experiment also shows that a slightly different pump beam will change the power distributions between the different SH components.

In conclusion, we presented the first experimental observation of self-accelerating nonlinear beams in quadratic media. We showed that nonlinearly coupled beams of different frequencies exhibit shape-preserving acceleration inside a nonlinear medium which supports their coupling. The FH and SH exhibit joint self-similar acceleration within the nonlinear medium, but with intensity peaks that are asynchronous with respect to one another. The experimental results fully agree with the theoretical analysis in the 1D case [18] but unravel new phenomena in the 2D case. We also demonstrated the impact of self-healing
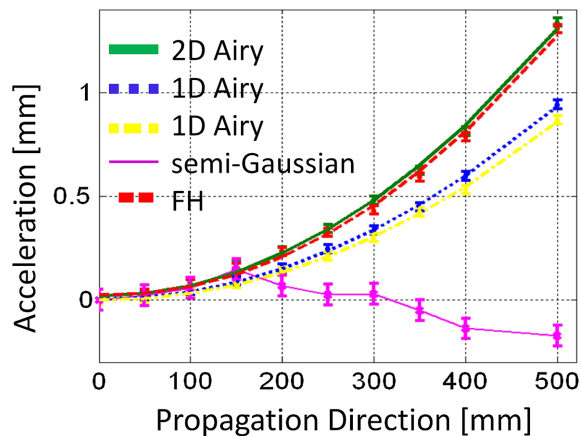

FIG. 3 (color online). Acceleration path of the SH beam components emerging when a 2D FH Airy beam is launched into the nonlinear crystal. As shown here, the 2D FH and 2D SH Airy beams are jointly accelerating.
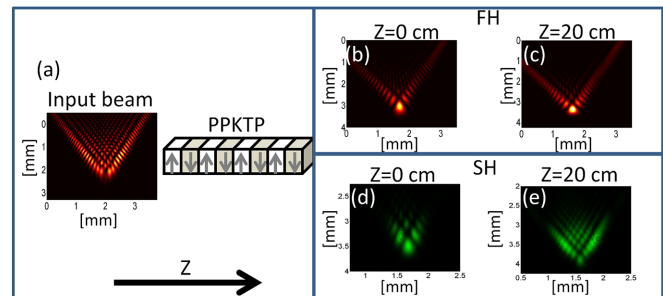

FIG. 4 (color online). FH, red; SH, green. Demonstration of the self-healing properties of a 2D FH and SH beam. The input pump is a 2D Airy beam with the main lobe blocked (a). The FH (b),(c) and the SH (d),(e) beams at the end of the nonlinear crystal and after 20 cm, respectively.

effects on the jointly accelerating beams, indicating the shape-preserving nature of these beams and the importance of the initial conditions (i.e., the pump beam), in the nonlinear dynamics of the system. It would be interesting to expand this work to study the nonlinear evolution of other types of self-accelerating beams such as parabolic beams [21] or circular Airy beams [22]. In addition, whereas our measurements were done at relatively low pump power, accelerating quadratic solitons should be observed at higher pump powers [16,17].

*Corresponding author.
ady@post.tau.ac.il

[1] M. V. Berry and N. L. Balazs, Am. J. Phys. **47,** 264 (1979).
[2] G. A. Siviloglou and D. N. Christodoulides, Opt. Lett. **32,** 979 (2007).
[3] G. A. Siviloglou et al., Phys. Rev. Lett. **99,** 213901 (2007).
[4] G. A. Siviloglou et al., Opt. Lett. **33,** 207 (2008).
[5] E. Greenfield et al., Phys. Rev. Lett. **106,** 213902 (2011); L. Froehly et al., Opt. Express **19,** 16 455 (2011).
[6] J. Baumgartl, M. Mazilu, and K. Dholakia, Nature Photon. **2,** 675 (2008).
[7] P. Polynkin et al., Science **324,** 229 (2009).
[8] A. Chong, W. H. Renninger, D. N. Christodoulides and F. W. Wise, Nature Photon. **4,** 103 (2010).
[9] D. Abdollahpour et al., Phys. Rev. Lett. **105,** 253901 (2010).
[10] T. Ellenbogen et al., Nature Photon. **3,** 395 (2009).
[11] I. Dolev et al., Appl. Phys. Lett. **95,** 201112 (2009).
[12] I. Dolev, T. Ellenbogen, and A. Arie, Opt. Lett. **35,** 1581 (2010).
[13] I. Dolev and A. Arie, Appl. Phys. Lett. **97,** 171102 (2010).
[14] S. Jia et al., Phys. Rev. Lett. **104,** 253904 (2010).
[15] Y. Hu et al., Opt. Lett. **35,** 3952 (2010).
[16] Y. N. Karamzin and A. P. Sukhorukov, Sov. Phys. JETP **20,** 339 (1974).
[17] W. E. Torruellas et al., Phys. Rev. Lett. **74,** 5036 (1995).
[18] I. Kaminer, M. Segev, and D. N. Christodoulides, Phys. Rev. Lett. **106,** 213903 (2011).
[19] W. Lee, Appl. Opt. **18,** 3661 (1979).
[20] M. M. Fejer et al., IEEE J. Quantum Electron. **28,** 2631 (1992).
[21] M. A. Bandres, Opt. Lett. **33,** 1678 (2008).
[22] N. K. Efremidis and D. N. Christodoulides, Opt. Lett. **35,** 4045 (2010).